

Anal Chem. Author manuscript; available in PMC 2012 September 15.

Published in final edited form as:

Anal Chem. 2011 September 15; 83(18): 7173-7178. doi:10.1021/ac2016085.

Quantitative Label-Free Characterization of Avidin-Biotin Assemblies on Silanized Glass

Li-Jung Chen¹, Jeong Hyun Seo², Michael J. Eller¹, Stanislav V. Verkhoturov¹, Sunny S. Shah², Alexander Revzin², and Emile A. Schweikert^{1,*}

¹Department of Chemistry, Texas A&M University, College Station, TX, USA

²Department of Biomedical Engineering, University of California, Davis, CA, USA

Abstract

In this study, a ToF-SIMS operating in the event-by-event bombardment/detection mode was used to characterize avidin-biotin assemblies on silane-modified glass substrates. SIMS was used to analyze several variants of the biointerface, including avidin physically adsorbed on a monofunctional acryl silane surface and covalently attached on a mono-functional (amine terminated) and a bi-functional (amine and acryl terminated) silanes. The goal of these studies was to determine density of avidin and biotin layers chemical or physically adsorbed on silanized glass substrate. An individual impact of a C₆₀ projectile used in this study creates a hemispherical crater (~10 nm in diameter) and emits large numbers of secondary ions from the same nanovolume. Thus, a single impact enables to unfold distinct secondary ions that span the thickness of the assembled film. This method was used to monitor presence of glass, silane and protein ions and to estimate the thickness and density of the avidin layer. In addition, we employed double coincidence mass spectrometry approach to identify ions co-emitted from a specific stratum of the biointerface. This approach was used to determine density of biotin and avidin immobilization while eliminating interferences from isobaric ions that originated from other constituents on the surface. Overall, novel ToF-SIMS quantitative approaches employed here were useful for examining complex biointerface and determining both lateral and in depth composition of the film.

Keywords

ToF-SIMS; C₆₀ primary ions; Avidin and biotin; event-by-event bombardment/detection; double coincidence mass spectrometry

INTRODUCTION

The avidin-biotin interaction is one of the most common strategies for conjugating biomolecules like enzymes, antibodies or chemokines onto surfaces and carries high significance for cell/tissue engineering and biosensing applications. ¹⁻⁵ Notably, the biotinylated molecules can be immobilized on a silanized surface and hence fashioned in micropatterns. ⁶⁻⁷ Our laboratories have been interested in employing silanized glass or indium tin oxide (ITO, or tin-doped indium oxide) substrates for cell micropatterning and immunosensor development. ⁸⁻¹¹ In the past we have relied on physical adsorption of antibodies in designing micropatterned immunoassays for cytokine detection; however, these immunosensors were insufficiently sensitive compared to standard ELISA. We hypothesize that improvement in performance of these biosensors may be achieved by

^{*}schweikert@mail.chem.tamu.edu .

oriented attachment of antibodies onto surface via avidin-biotin interactions. In the present paper we focus on characterizing the avidin layer assembled on glass as this layer represents an important building block in construction of biosensing surfaces.

Another important parameter investigated in this paper is the effect of silane composition on the quality/density of the assembled avidin-biotin layer. In the past, we have made extensive use of hydrogel micropatterning in designing surfaces for cell cultivation and biosensing. ¹¹⁻¹³ In this micropatterning strategy acrylated silanes are used for anchoring gel structures onto glass substrates. While providing an excellent coupling layer for gel attachment, acrylated silanes can only be used for physical and not covalent adsorption of biomolecules. One way to enhance functionality of the surface is to create a bi-functional silane layer containing end groups for gel and protein attachment. ¹⁴ The development of silanized surfaces for miropatterning of both proteins and hydrogels is the future goal. In the present paper, we compared avidin-biotin assembly on a bi-functional layer of amine- and acryl-terminated silane molecules to avidin-biotin attachment on mono-function silanes containing either acryl or amine terminal groups.

Relevant testing can be accomplished with fluorescent microscopy or imaging mass spectrometry where the avidin is either tagged with a dye or isotopically labeled. 6,15 We present here a label-free method for the quantification of the avidin-biotin complex and examine also its immobilization density vs. the silane functionality used for surface attachment. Our approach relies on time-of-flight secondary ion mass spectrometry, ToF-SIMS, with C_{60} as projectiles. The experiments are run in the event-by-event bombardment-detection mode, where the ionized ejecta from a single projectile impact are recorded individually. $^{16-17}$ It has been shown experimentally and by molecular dynamics simulations that the impact of one C_{60} of a few tens of keV generates secondary ion (SI) emission from an area of ~ 10 nm in diameter and a depth of 5-10 nm. 18 To obtain statistically valid information on such a nanovolume, we run a sequence of single C_{60} impacts in stochastic fashion on a sampling area, and subsequently compile the individual SI records and investigate similarities. The result is spatially refined molecular information in a non-imaging mode. The performance of event-by-event ToF-SIMS is illustrated below.

MATERIALS AND METHODS

Materials

Glass slides $(75 \times 25 \text{ mm}^2)$ were obtained from VWR (West Chester, PA). (3-Acryloxypropyl) trimethoxysilane and N-(2-aminoethyl)-3-aminopropyl trimethoxysilane were purchased from Gelest, Inc. (Morisville, PA). 2-hydroxy-2-methylpropiophenone (photoinitiator), dimethylsulfoxide (DMSO), and anhydrous toluene (99.9%) were purchased from Sigma-Aldrich (Saint Louis, MO). NHS-dPEG®12-biotin was purchased from Quanta Biodesign, Ltd. (Powell, OH). NeutrAvidin® was purchased from Invitrogen (Carlsbad, CA).

Surface Preparation

The glass slides were immersed for 10 min into piranha solution consisting of a 1:1 ratio of 95% (v/v) and 35% (w/v) sulfuric acid. The glass slides were then thoroughly rinsed with deionized (DI) water, dried with nitrogen and stored under in class 10,000 cleanroom until further use. For silane modification, the glass slides were treated with oxygen plasma (YES-R3, San Jose, CA) at 300 W for 5 min and then immersed in silane solution. Three types of silanizations were performed; glass substrates were immersed in: (1) 0.1% v/v (3-acryloxypropyl) trimethoxysilane (acryl silane), (2) 0.1% v/v (2-aminoethyl)-3-aminopropyl trimethoxysilane (NH₂ silane), and (3) a mixture of (3-acryloxypropyl) trimethoxysilane and

(2-aminoethyl)-3-aminopropyl trimethoxysilane prepared at 0.2% v/v. All silanes were prepared in anhydrous toluene and were reacted with surfaces for 5 h in a glove bag filled with nitrogen. After silanization reaction, slides were rinsed with fresh toluene, dried under nitrogen, and baked at 100 °C for 1 h. The silane-modified glass slides were stored in a desiccator before use.

As a first step in bio-functionalization surfaces were treated in 250 mM NHS-dPEG12-biotin prepared in 1:1 mixture of DMSO and phosphate buffered saline (PBS) for 1 h, in which the NHS ester group can react with the surface NH_2 group by nucleophilic attack and produce a stable amide bond (-NH-CO-, Figure 1(a))¹⁹. Subsequently surfaces were rinsed with PBS buffer and distilled water to remove unreacted linker, and then incubated in 1mg/mL of neutravidin for 1 h (neutravidin can easily interact with biotin on the surface, Figure 1(b)).

Cluster C₆₀^{1,2+} ToF-SIMS

The secondary ion mass spectrometry measurements were carried out with a custom-built secondary ion mass spectrometer coupled with time of flight mass analyzer (ToF-SIMS). Cluster C_{60} ToF-SIMS used in our laboratory produces $C_{60}^{1,2+}$ projectiles with total impact energy on the target sample of 26 keV and 43 keV. $^{20-22}$ Briefly, the neutral C_{60} powder is heated until it sublimes. The effusion C_{60} vapor is then ionized by electron impact ionization to yield charged C_{60} ions. The singly and doubly charged C_{60} ions of interest were mass-selected by a Wien filter. Electrostatic lenses were used to focus and steer primary $C_{60}^{1,2+}$ ions toward an off-center aperture that can deflect ions and prevent neutrals from impacting samples. The ToF-SIMS measurement involves the collection of the start signal triggered by the emitted electron from the impacted site. The emitted secondary ions were recorded simultaneously with a micro channel plate (MCP) detector (stop signal) and results in a negative ion mass spectrum. The ToF-SIMS measurement allows for the effective detection of secondary ions in the mass range of m/z 0-1500.

Individual Cluster Impact ToF-SIMS

A single event is defined as one primary ion impact on target sample followed by emissions of secondary ions and detection. In the event-by-event bombardment-detection mode, each individual event is separated in time and space and recorded individually. ¹⁶ The time spent for data acquisition of ~5 million events is ~80 minutes with the acquisition rate of ~1000 C_{60} impacts/s in the event-by-event bombardment/detection mode. A coincidental ion mass spectrum is generated by selecting an ion of interest and recording the collection of all coemitted secondary ions under individual projectile impacts. The coincidence secondary ion spectrum contains the record of co-localized secondary ions emitted from a given nanovolume after each individual impact.

As shown in Figures 1(a) and (b), the size of the avidin-biotin complex is well suited for a chemical mapping study by using ToF-SIMS in the event-by-event bombardment/detection mode. The compound thickness of avidin-biotin and silanes layers was ~10-12 nm whereas the sampling depth of cluster ToF-SIMS was 5-10 nm (~10 nm in diameter hemispherical nanovolume).

SIMS analysis was used to characterize surface composition at each step in the surface modification: after silane assembly, biotin-PEG-NHS attachment and avidin conjugation. The first test case is the glass surface modified with an amino silane. Then the biotin with the functional group the (PEG)₁₂-NHS linker was immobilized on the amino silane with the leaving group succinimide NHS. Lastly, the avidin was immobilized on a biotin-(PEG)₁₂-NHS linker.

RESULTS AND DISCUSSION

A key performance parameter in the biosensing application is the effect of silane composition on the density of the attached avidin-biotin complex.

Figure 2 shows the secondary ion mass spectra of biotin-(PEG) $_{12}$ -NHS linker (biotin linker or BL) on amino silane (Fig. 2(a)) and avidin immobilized on a biotin-(PEG) $_{12}$ -NHS modified amino silane (Fig. 2(b)) respectively. The mass spectra show that the negative ions at m/z 91 ([CH $_2$ C $_6$ H $_5$] $^-$, side chain of Phenylalanine) and m/z 107 ([CH $_2$ C $_6$ H $_4$ OH] $^-$, side chain of Tyrosine) are distinct peaks for the avidin. The intensities of biotin-(PEG) $_{12}$ -NHS characteristic ions found at m/z 183, 209, 211, 225, 267, 311, 325 and 339 decrease notably after the addition of avidin (Fig. 2 (b)). As shown in the schematic Figure 1(b), the lower yields of biotin-(PEG) $_{12}$ -NHS peaks in the mass spectra are attributed to the thick layer of avidin (5-7nm), which reduces secondary ion emission from the underlying biotin-(PEG) $_{12}$ -NHS layer.

In addition, Figure 2(b) shows lower glass and silane-related peaks at m/z 77 (SiO₂)OH⁻, 121 (SiO₂)₂H⁻, 137 (SiO₂)₂OH⁻, and 197 (SiO₂)₃OH⁻. After adding avidin, the low glass-related signals indicate that the entire surface was covered with avidin, thus reducing emission of SI from the underlying glass substrate. In contrast, Figure 1(a) shows that the thickness of biotin and silane layers is smaller than the depth of projectile impact which resulted in the higher intensities of biotin, silane and glass correlated peaks.

The data can be assessed in a quantitative manner with the SI yield, Y_A (%) which is determined as follows:

$$Y_A$$
 (%) = 100 $\left(\frac{N_A}{N_0}\right)$ = 100 $\left(P_A\right)$ = 100 $\left(\frac{I_A - I_{BG}}{N_0}\right)$ Eq. (1)

where N_A is the number of impacts/events when ion A was detected; N_0 is the total number of projectile impacts/events; P_A is the probability of detected secondary ions per single projectile impact which corresponds to NA / N_0 , for small yields ($Y_A < 100\%$); I_A is the secondary ion intensity while I_{BG} is the intensity of background. The secondary ion yield is expressed as the measured peak area under ion A subtracts the background area measured in the mass spectrum and then divided by the total number of projectile impacts.

Table 1 lists the SI yields of characteristic fragments for avidin and biotin complexes on various silanes. The doubly charged C_{60} (total energy 43 keV) shows significantly higher yields than the singly charged C_{60} (total energy 26 keV).²³ The higher molecular ion yields facilitate the identification of specific ions from bio-complexes. In particular, they enhance the coincidental secondary ion signals and hence the higher probability of co-emission of secondary ions with a selected ion.

The SI yields for the avidin-related fragment ions at m/z 91 and 107 are listed for the assemblies immobilized with different silanes (Table 1). The corresponding mass spectra (Figure 3) show that the abundance of the fragment ions of the phenylalanine (Phe) and tyrosine (Tyr) correlates with that of the glass-related signals. Lower substrate signals (Figure 3) signify better covalent binding between NH $_2$ silane and biotin-(PEG) $_{12}$ -NHS that yields higher avidin intensity. A more reactive NH $_2$ silane and biotin-(PEG) $_{12}$ -NHS interface thus provides a better binding performance with avidin.

The low intensity of glass/silane fragments (Figure 3) in the mass spectrum of NH₂ silane case is attributed to the small amount of avidin defects on the entire surface. The reactivity

variation by the types of silanes influences the biotin immobilization performance between silanes and biotin. In both test cases of avidin and biotin immobilized on acryl silane and mixed (acryl and NH₂) silane, the higher signals of glass-related peaks at m/z 121 (SiO₂)₂H⁻ and 137 (SiO₂)₂OH⁻ indicate a larger amount of defects in avidin immobilization resulting in the enhanced possibility of SI emission from the substrate. Also, in the test case of acrylated silane, signals corresponding to the biotin-(PEG)₁₂-NHS fragments at m/z 183 and 311, 325, and 339 are lower than those on NH₂ and mixed (NH₂ and acrylated) silanes. This observation is reasonable given the higher density of NH₂ groups available in the mono-functional silane layer for reaction with NHS moieties on biotin. In contrast, interaction of biotin-(PEG)₁₂-NHS with acrylated silane resulted in a weak signal suggesting that only a limited number of biotins were physically bound on this silane layer. Subsequent incubation of the surface with avidin resulted in a low protein signal. These studies highlight the benefits of covalent attachment in creating a dense avidin layer on the surface.

However, the relative SI yields cannot be directly correlated with the degree of surface coverage because of the inhomogeneous surfaces as sketched in Figures 4(a) and (b). The irregular coverage of avidin and biotin results in unequal impacts/emissions from the same sample. Table 1 shows similar yields in avidin (at m/z 91 and 107) for all test cases. The apparent higher yields at m/z 137 (glass), 183 and 311 (biotin-(PEG)₁₂-NHS) of the avidin biotin on acrylated silane implicate the presence of avidin defects.

The SI yields provide a rough comparison of the attachment of the complexes. A quantitative method for determining their binding densities which takes into account the fractional coverage of the immobilized amounts of avidin and biotin is described below.

As noted at the outset, the event-by-event ToF-SIMS method allows to select a specific ion and to identify the co-emitted SIs which originate from molecules co-located in the nanovolume with the selected ion. Figures 5 show the secondary ions co-emitted with m/z 422 from the biotin- $(PEG)_{12}$ -NHS linker and hence the molecular ions co-located in the nano-domain. Peaks related to the biotin- $(PEG)_{12}$ -NHS linker at m/z 183 and 325 were both observed (Figure 5(a) and (b)). In comparison, Figure 5(b) shows the characteristic peaks of avidin at m/z 91 (Phe) and 107 (Tyr).

The absence of glass-related peaks at m/z 121 (SiO₂)₂H⁻ and 137 (SiO₂)₂OH⁻ (seen in Figure 5(b)) indicates that the layers of avidin (5-7 nm) and biotin-(PEG)₁₂-NHS linker (~5 nm) limit the SI emission from the underlying glass substrate. It may be recalled that the emission nanovolume of secondary ions is about 5-10 nm in depth. Thus, the majority of chemical signals shown in Figure 5(b) are from avidin and biotin conjugates. Nevertheless, the inhomogeneous surface generates various types of projectile impacts/emissions. Thus, the single coincidence spectrum of ions co-emitted with m/z 422 may contain ions at m/z 75 from both avidin and silane. Figure 6 sketches the types of impacts on a complex surface. Overlapping ions at m/z 75 can be resolved via double coincidence, i.e. by selecting events of co-emission of specific ions from avidin and biotin.²⁴

Figure 7 shows the comparison of single coincidence and double coincidence ion mass spectra. In the double coincidence spectrum, the ratio of the peaks at m/z 75 and 74 is lower than that in the single coincidence spectrum and original mass spectrum. Secondary ions at m/z 75 could originate from both silane (CH₃SiO₂⁻) and avidin (Methionine, Met) respectively. Two coincidence windows were set with ions from biotin-(PEG)₁₂-NHS at m/z 183 and avidin at m/z 91 (Figure 7(b)). Only those ions co-emitted with both ions at m/z 183 and 91 can be present in the double coincidence spectrum, impacts yielding interfering ions at m/z 75 from silane were eliminated. Other interfering ions at m/z 197 observed in original mass spectra were determined as ions related to both biotin-(PEG)₁₂-NHS linker and glass.

The double coincidence methodology with co-emitted ions of avidin and biotin layer has removed the interfering glass-related peaks.

The double coincidental ion mass spectra arise for a specific chemical distribution of the ligand and protein molecules residing on the topmost layer of the biointerface. The event-by-event bombardment/detection mode allows to deconvolute signals emanating from complex inhomogeneous biointerfaces and to extract a spatially distributed mass spectrum originating from avidin and biotin conjugates.

A further application of the coincidence mode is to quantify the fractional surface coverage of avidin. As described above, differences in silane composition affect attachment of the biotin- $(PEG)_{12}$ -NHS molecules, and ultimately determine the quality of the topmost avidin layer. We noted earlier, the absence of glass-related peaks in the NH₂ silane and the presence of prominent glass peaks in acrylated silane suggesting different degrees of immobilization for avidin. The hypothesis is that the avidin coverage on the NH₂ silane is greater than acrylated silane. The ability to test the avidin surface density will in turn allow us to assess the quality and quantity of protein immobilization.

The surface density can be expressed as the fractional coverage, which is computed from the ratio between the numbers of effective impacts on an immobilized specimen to that of total primary ions sent to bombard a target surface.²⁵⁻²⁶ The derivation of the number of effective impacts is described as follows:

Number of effective impacts

As shown in the coincidental mass spectrum, more than one ion is detected from a single projectile impact. When two ions are co-emitted independently, i.e. the emission of ion A does not affect the emission of ion B, the probability of co-emitted ions A and B ($P_{A,B}$) is statistically equal to the product of individual probability of ion A (P_A) and ion B (P_B):

$$P_{A,B} = P_A P_B$$
 Eq.(2)

As described earlier, the secondary ion yield is correlated to the probability. Thus, the relationship of co-emitted ions can be defined by:

$$Y_{A,B} = Y_A Y_B$$
 Eq.(3)

where $Y_{A,B}$ is the coincidental yield when ions A and B are detected simultaneously under a single projectile impact, Y_A is the secondary ion yield of ion A while Y_B is the secondary ion yield of ion B. Considering the distribution of covered species, the number of projectile impacts should be replaced as the number of effective impacts on the species. To obtain the number of effective impact, the equation is deduced from Eq.(3) as follows:

$$\frac{I_{A,B}}{N_{eff}} = \left(\frac{I_A}{N_{eff}}\right) \left(\frac{I_B}{N_{eff}}\right)$$
Eq.(4)

where $I_{A,B}$ is measured under the coincidental ion mass spectrum when ion A is co-emitted with ion B. I_A is measured at ion A peak area under the original secondary ion mass spectrum while I_B is measured from the ion B peak area. N_{eff} is the number of effective projectile impact on the specimen that generates ions A and B. Thus, the fractional coverage K(%) of a specimen can be obtained as the number of effective impacts (N_{eff}) divided by the total number of projectile sent to bombard on the sample target (N_0):

$$K(\%) = 100 \frac{N_{eff}}{N_0}$$
 Eq.(5)

In the present case, two co-emitted secondary ions are used to calculate the effective number of impacts on either biotin-(PEG)₁₂-NHS linker or avidin (Eq.(4)). For example, the coincidental intensity of ions at m/z 183 and 325 from biotin and ions at m/z 91 co-emitted with ions at m/z 107 from avidin were used. The fractional surface coverage K(%) is calculated using Eq.(5).

Table 2 lists the quantitative results of the degree of biotin- $(PEG)_{12}$ -NHS and avidin densities of immobilization on various silanes. An immobilization density of ~82% was obtained for the biotin- $(PEG)_{12}$ -NHS linker on NH₂ silanes. The corresponding numbers are 83% for the mixed (NH₂ and acryl) silane and 61% for the acryl silane. Interestingly, the density of avidin attachment on NH₂ silane is ~100%. We noted earlier the absence of glass-related peaks in these samples, indeed due to the high avidin immobilization density. In the test case of acryl silane, the avidin density is of ~39% while it is ~54% for mixed silanes. The low degree of avidin attachment on acryl silane may be explained by the lower density of biotin molecules mentioned earlier, but also by the disoriented physical adsorption of these molecules which makes for less effective avidin-biotin conjugation. As shown by our data, mixed silanes containing acrylate and amine functionalities had intermediate coverage of avidin suggesting once again that covalent attachment to amine moieties is an important determinant of the quality of the avidin layer.

Tests with biotin-(PEG) $_{12}$ -NHS only on various silanes gave similar results from the acrylated silane. Only 22% of biotin linker was attached on the acrylated silane functionalized surface whereas the biotin binding densities were of 84% and 82% for the NH $_2$ and mixed silane respectively.

In addition, we compared the binding density of avidin on different silanes as listed in the last column (Table 2). While avidin attached on the silanized surface without a biotin linker, it shows better attachment with NH₂ silanes in comparison to acrylated and mixed silanes. Nevertheless, the avidin densities are lower than those mediated with the biotin linker. The quantitative results demonstrate the importance of the biotin linker in the layer-by-layer assemblies. Also, various functionalities of silanes influence the biotin linker binding performance that changes the binding densities of attached avidin.

CONCLUSIONS

This work shows the feasibility of applying cluster C_{60} ToF-SIMS with the event-by-event bombardment/detection mode to differentiate the characteristic peaks for intact avidin-biotin complex. The qualitative information shows the effect of novel bifunctional silanes on the density of avidin-biotin immobilization. The double coincidence enhances the accuracy of identifying distinct peaks of avidin-biotin biointerface. Also, the capability of quantifying the biocomplexes enables to evaluate the effect of various silane compositions on the density of avidin-biotin attachment. This label-free mass spectrometric methodology offers both qualitative and quantitative means of investigating the amounts of biomolecules immobilized on silanized surfaces. The double coincidence label-free detection might further contribute to ToF-SIMS imaging of avidin-biotin complexes.

Acknowledgments

This work was supported by the grants from the National Science Foundation (Grant-CHE 0750377 to EAS) and the National Institutes of Health (Grant-EB 006519 to AR).

REFERENCES

(1). Osterfeld SJ, Yu H, Gaster RS, Caramuta S, Xu L, Han SJ, Hall DA, Wilson RJ, Sun SH, White RL, Davis RW, Pourmand N, Wang SX. P Natl Acad Sci USA. 2008; 105:20637.

- (2). Gunnarsson A, Sjovall P, Hook F. Nano Lett. 2010; 10:732. [PubMed: 20085369]
- (3). Tiefenauer L, Ros R. Colloid Surf. B-Biointerfaces. 2002; 23:95.
- (4). Pei RJ, Cheng ZL, Wang EK, Yang XR. Biosens Bioelectron. 2001; 16:355. [PubMed: 11672649]
- (5). Afonso C, Fenselau C. Anal Chem. 2003; 75:694. [PubMed: 12585503]
- (6). Dubey M, Emoto K, Takahashi H, Castner DG, Grainger DW. Adv Funct Mater. 2009; 19:3046.
- (7). Dubey M, Emoto K, Cheng F, Gamble LJ, Takahashi H, Grainger DW, Castner DG. Surface and Interface Analysis. 2009; 41:645. [PubMed: 19756241]
- (8). Shah SS, Howland MC, Chen LJ, Silangcruz J, Verkhoturov SV, Schweikert EA, Parikh AN, Revzin A. Acs Appl Mater Inter. 2009; 1:2592.
- (9). Shah SS, Lee JY, Verkhoturov S, Tuleuova N, Schweikert EA, Ramanculov E, Revzin A. Langmuir. 2008; 24:6837. [PubMed: 18512875]
- (10). Chen LJ, Shah SS, Verkhoturov SV, Revzin A, Schweikert EA. Surface and Interface Analysis. 2011; 43:555. [PubMed: 21278908]
- (11). Zhu H, Stybayeva G, Silangcruz J, Yan J, Ramanculov E, Dandekar S, George MD, Revzin A. Anal Chem. 2009; 81:8150. [PubMed: 19739655]
- (12). Revzin A, Tompkins RG, Toner M. Langmuir. 2003; 19:9855.
- (13). Lee JY, Shah SS, Yan J, Howland MC, Parikh AN, Pan TR, Revzin A. Langmuir. 2009; 25:3880. [PubMed: 19275186]
- (14). Lee KB, Jung YH, Lee ZW, Kim S, Choi IS. Biomaterials. 2007; 28:5594. [PubMed: 17869337]
- (15). Belu AM, Yang ZP, Aslami R, Chilkoti A. Anal Chem. 2001; 73:143. [PubMed: 11199958]
- (16). Park MA, Gibson KA, Quinones L, Schweikert EA. Science. 1990; 248:988. [PubMed: 17745403]
- (17). Rickman RD, Verkhoturov SV, Parilis ES, Schweikert EA. Phys. Rev. Lett. 2004; 92
- (18). Li Z, Verkhoturov SV, Locklear JE, Schweikert EA. Int J Mass Spectrom. 2008; 269:112.
- (19). Hermanson, GT. Bioconjugate techniques. 2nd ed. Elsevier Academic Press; Amsterdam; Boston: 2008.
- (20). Locklear, JE. Ph. D. Dissertation. Texas A&M University; 2006.
- (21). Eller MJ, Verkhoturov SV, Della-Negra S, Rickman RD, Schweikert EA. Surface and Interface Analysis. 2011; 43:484.
- (22). Verkhoturov SV, Eller MJ, Rickman RD, Della-Negra S, Schweikert EA. J Phys Chem C. 2010; 114:5637.
- (23). Fernandez-Lima FA, Eller MJ, Verkhoturov SV, Della-Negra S, Schweikert EA. J Phys Chem Lett. 2010; 1:3510. [PubMed: 21218166]
- (24). Ray KB, Park MA, Schweikert EA. Nucl Instrum Meth B. 1993; 82:317.
- (25). Raiagopalachary S, Verkhoturov SV, Schweikert EA. Anal Chem. 2009; 81:1089. [PubMed: 19105605]
- (26). Pinnick VT, Verkhoturov SV, Kaledin L, Bisrat Y, Schweikert EA. Anal Chem. 2009; 81:7527. [PubMed: 19655772]

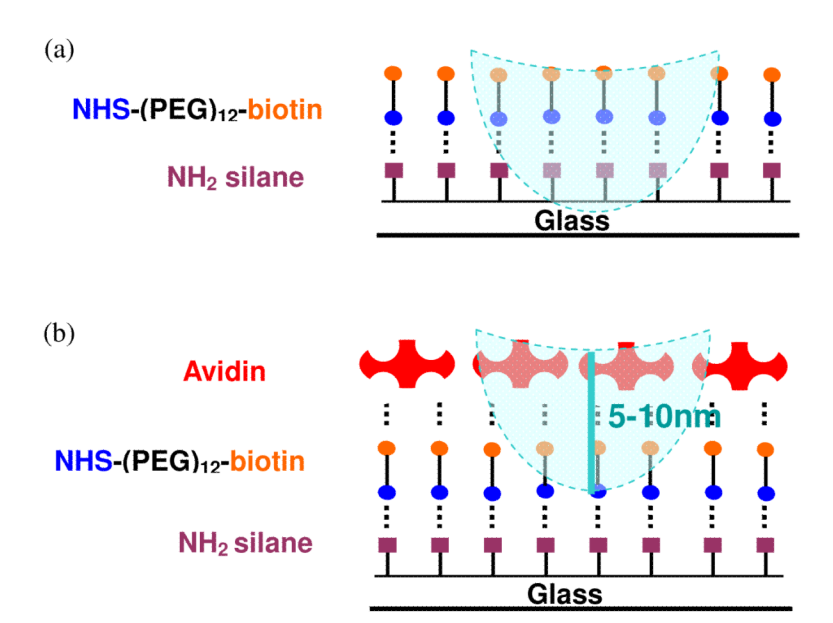


Figure 1. The depth of emission of individual C_{60} projectiles impacts on: (a) NHS-(PEG)₁₂-biotin modified on NH₂ silane surface; (b) avidin immobilized on NHS-(PEG)₁₂-biotin modified NH₂ silane surface.

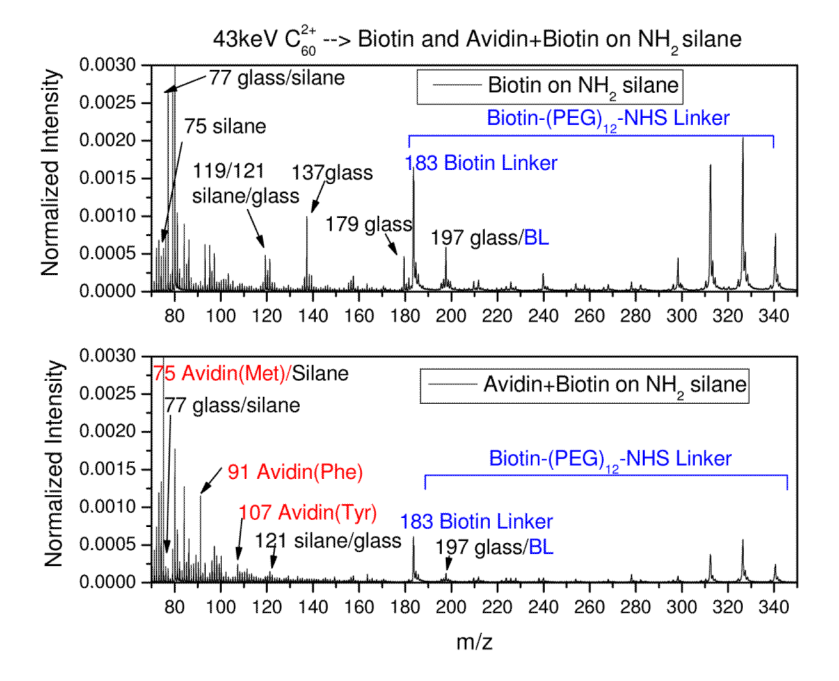


Figure 2.The secondary ion mass spectra: (a) biotin immobilized on the amino silane modified glass surface; (b) avidin attached on the biotin immobilized amino silane modified glass surface.

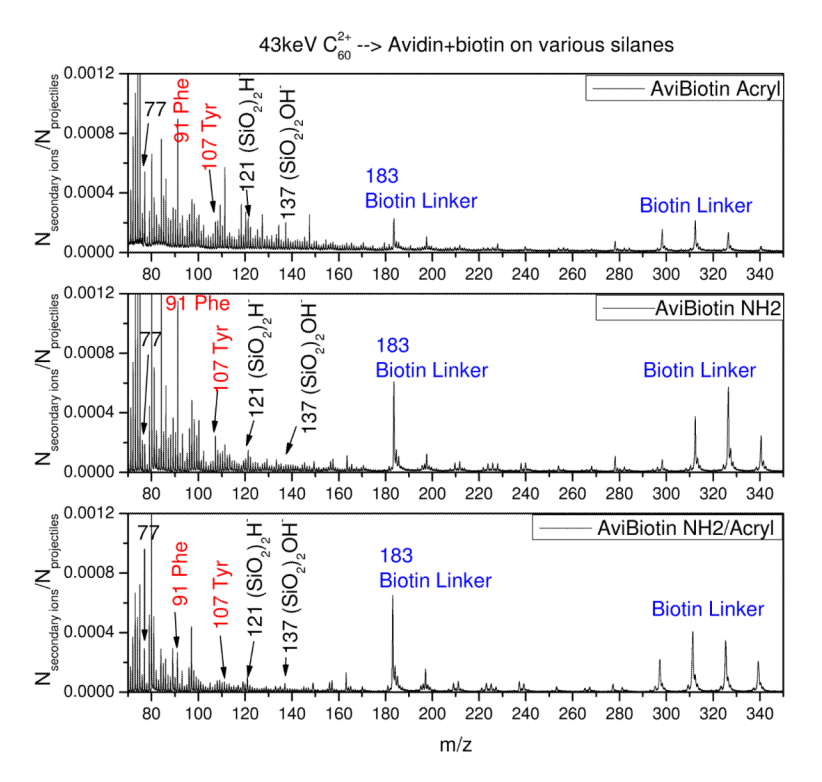


Figure 3.The secondary ion mass spectra of avidin and biotin linker attached respectively on acryl, amino, and amino/acryl mixed silanes.

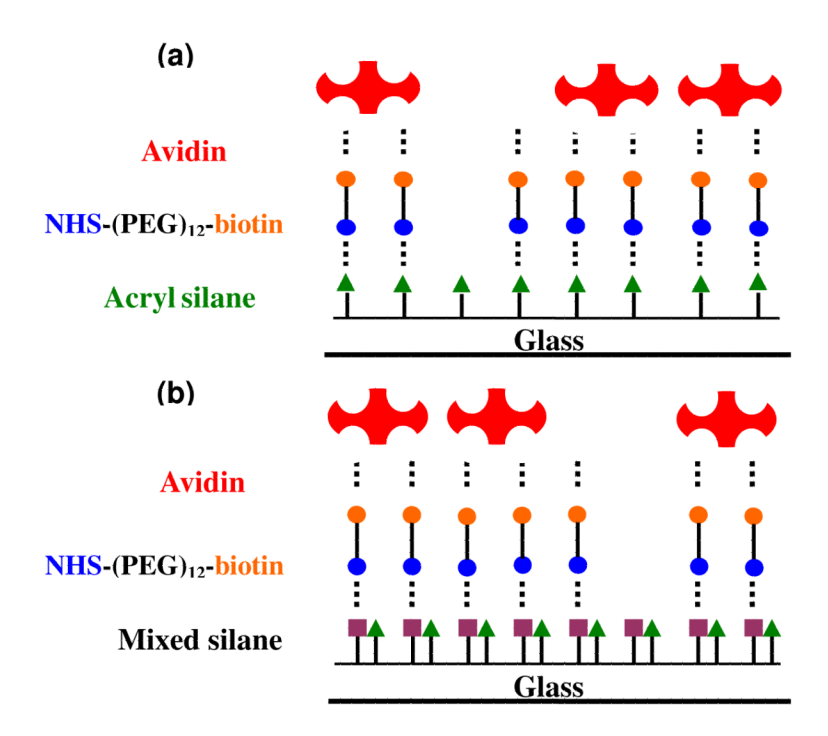


Figure 4.The schematic of irregular coating of avidin and biotin on: (a) acryl silanized glass surface; (b) mixed (acryl and amino silanes) silanized surface.

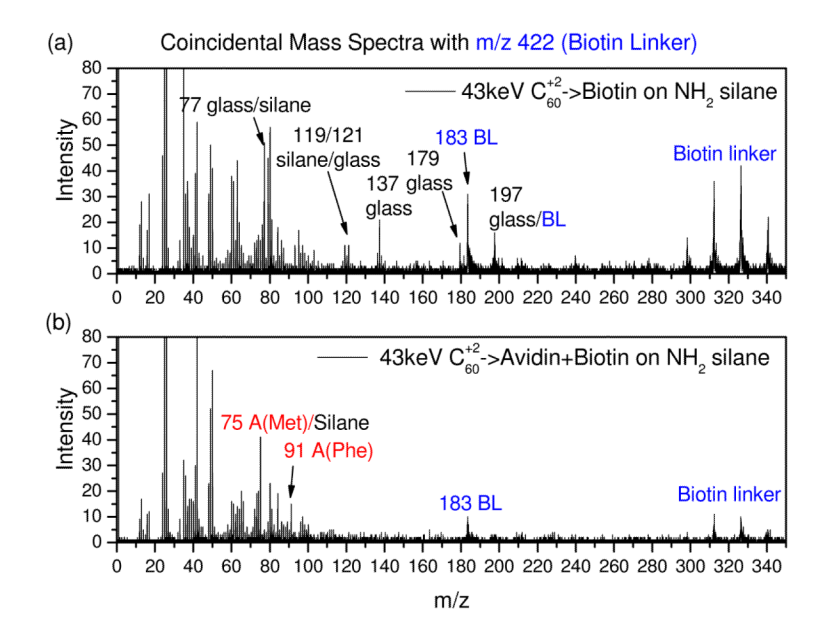


Figure 5. Coincidental spectra with co-emitted secondary ions with ion at m/z 422 from biotin- $(PEG)_{12}$ -NHS linker. (a) biotin- $(PEG)_{12}$ -NHS on NH₂ silane; (b) Avidin+biotin- $(PEG)_{12}$ -NHS on NH₂ silane.

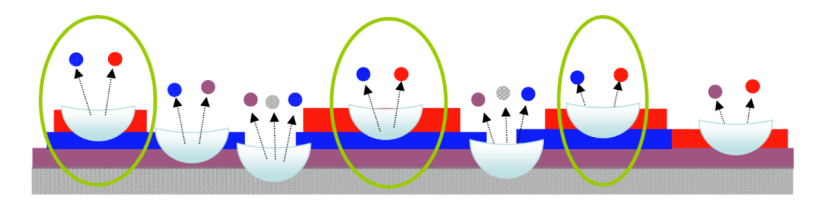


Figure 6.Diagram of co-emitted secondary ions from an avidin+biotin-(PEG)₁₂-NHS+NH₂ silane on glass surface. (Red: avidin; blue: biotin-(PEG)₁₂-NHS; purple: NH₂ silane; grey: glass)

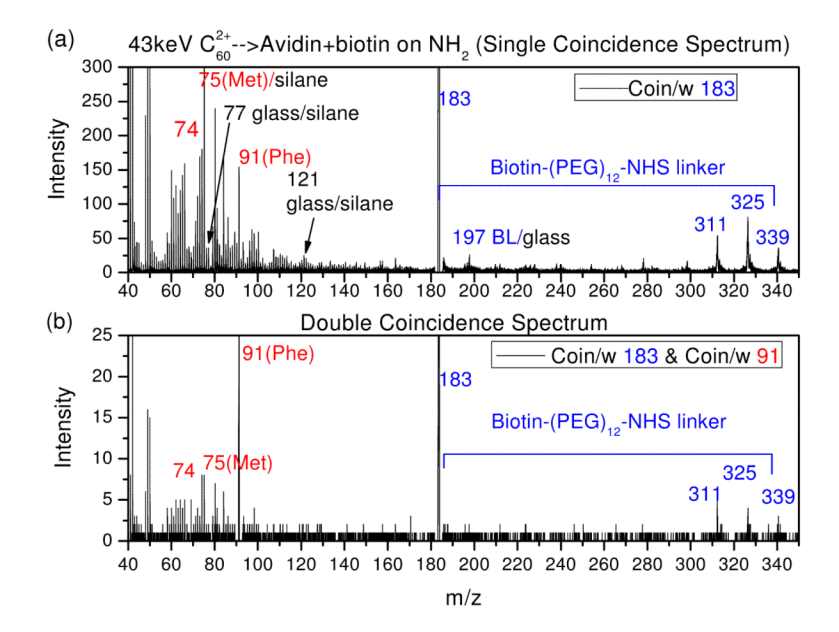


Figure 7. (a) Single coincidental ion mass spectrum with ion at m/z 183 from the biotin-(PEG)₁₂-NHS linker of sample avidin+biotin linker on NH₂ silane. (b) Double coincidental ion mass spectrum with two selected coincidental ions at m/z 183 (biotin linker) and m/z 91 (avidin) originate from sample avidin + biotin linker on NH₂ silane.

Tables 1

SI yields (%) of a vidin+ biotin on various silanes run with 26 keV C_{60}^+ and 43 keV C_{60}^{+2} bombardment

Chen et al.

26 keV C_{60}^+ Avidin Biotin on Various Silanes	Avidin Glass	8.9	3.9	6.0	9.0	0.2	0.4	0.2	0.1	0.1	1	;
	Mixed (NH ₂ &Acry)	7.0	3.3	6.0	0.3	0.3	0.2	0.1	0.1	0.1	1.0	8.0
	Acrylated Silane	12.5	5.5	1.9	1.3	0.2	0.6	0.2	0.1	0.1	0.2	0.1
	NH ₂ Silane	8.3	5.1	1.1	0.7	0.1	0.4	0.1	0.1	<0.1	0.4	0.3
	z/m	26	42	50	75	77	91	107	121	137	183	311
43 keV C_{60}^{+2} Avidin Biotin on Various Silanes	$\begin{array}{c} Mixed\\ (NH_2\&Acry) \end{array}$	26.3	10.3	5.0	3.5	9.0	1.3	0.3	0.4	0.1	3.2	1.7
	Acrylated Silane	42.4	15.0	8.0	4.0	6.0	1.5	0.3	0.5	0.5	0.8	8.0
	NH ₂ Silane	35.8	14.6	8.9	5.2	9.0	1.9	0.5	0.4	0.1	2.2	1.4
	m/z	26	42	50	75	77	91	107	121	137	183	311

Page 16

Table 2

The comparison of the binding densities of complex from samples: avidin with biotin-(PEG) $_{12}$ -NHS linker, biotin-(PEG) $_{12}$ -NHS linker, and avidin on various silanes.

Samples	Avidin + Bioti on various s		Biotin linker on silanes	Avidin on silanes	
Silanes	Biotin Linker Density (183,325)	Avidin Density (107,91)	Biotin Linker Density (183,325)	Avidin Density (107,91)	
NH ₂ Silane	82%	100%	84%	61%	
Acryl Silane	61%	39%	22%	54%	
Mixed Silane (NH ₂ : Acryl=1:1)	83%	54%	82%	44%	